Journal of Maps

ISSN: (Print) 1744-5647 (Online) Journal homepage: https://www.tandfonline.com/loi/tjom20

Stratigraphic framework of the late Miocene to Pliocene Pisco Formation at Cerro Colorado (Ica Desert, Peru)

C. Di Celma, E. Malinverno, K. Gariboldi, A. Gioncada, A. Rustichelli, P. P. Pierantoni, W. Landini, G. Bosio, C. Tinelli & G. Bianucci

To cite this article: C. Di Celma, E. Malinverno, K. Gariboldi, A. Gioncada, A. Rustichelli, P. P. Pierantoni, W. Landini, G. Bosio, C. Tinelli & G. Bianucci (2016) Stratigraphic framework of the late Miocene to Pliocene Pisco Formation at Cerro Colorado (Ica Desert, Peru), Journal of Maps, 12:3, 515-529, DOI: 10.1080/17445647.2015.1047906

To link to this article: https://doi.org/10.1080/17445647.2015.1047906

Journal of Maps, 2016
Vol. 12, No. 3, 515–529, http://dx.doi.org/10.1080/17445647.2015.1047906

Routledge
Taylor & Francis Group

SCIENCE

Stratigraphic framework of the late Miocene to Pliocene Pisco Formation at Cerro Colorado (Ica Desert, Peru)

C. Di Celma[a*], E. Malinverno[b], K. Gariboldi[c,d], A. Gioncada[c], A. Rustichelli[a], P. P. Pierantoni[a], W. Landini[c], G. Bosio[b], C. Tinelli[c] and G. Bianucci[c]

[a]*Scuola di Scienze e Tecnologie, Università di Camerino, Camerino, Italy;* [b]*Dipartimento di Scienze dell'Ambiente e del Territorio e di Scienze della Terra, Università di Milano-Bicocca, Milan, Italy;* [c]*Dipartimento di Scienze della Terra, Università di Pisa, Pisa, Italy;* [d]*Dottorato Regionale in Scienze della Terra Pegaso, Pisa, Italy*

(*Received 21 January 2015; resubmitted 22 April 2015; accepted 30 April 2015*)

This paper describes a ∼200 m-thick section of the Pisco Formation exposed at Cerro Colorado, an important fossiliferous site in the Ica desert. In order to properly place the fauna in its correct relative position, this study establishes the stratigraphic framework within which the different fossil-bearing intervals of this site can be compared and may prove invaluable in future high-resolution studies on the faunal change. Most of the Pisco Formation deposits exposed at Cerro Colorado consist of gently dipping fine-grained sandstones, diatomaceous siltstones and diatomites with minor ash layers and dolomites deposited within nearshore and offshore settings. To facilitate detailed stratigraphic correlations within the Pisco strata for a 30 km^2 area, eight marker beds have been defined and large-scale (1:10,000 scale) geological mapping conducted to determine fault positions, styles and offsets. The geological map shows that there are two important angular unconformities in the study area. The first one is the interformational basal unconformity of the Pisco Formation against folded, faulted, and planated Oligo-Miocene rocks of the Chilcatay Formation. The second is a low-angle intraformational erosional discontinuity of up to 4° angular discordance that allows the subdivision of the Pisco stratigraphy exposed in the study area into two informal allomembers. Dating of the exposed succession by diatom biostratigraphy suggests that the age of the lower allomember is late Miocene, whereas the upper allomember is late Miocene or younger.

Keywords: Pisco Formation; late Miocene; Cerro Colorado

1. Introduction

The late Oligocene to middle Miocene Chilcatay Formation and the late Miocene to Pliocene Pisco Formation of the Pisco basin, southern Peru, are characterized by an extraordinarily diverse vertebrate fossil fauna, including toothed whales, baleen whales, sea turtles, and fishes. Over the last 30 years this fauna has been documented in an enormous body of literature and, since 2006, thanks to an European collaboration involving Italian, Belgian, Dutch, French, and Peruvian researchers, a large number of fossil vertebrates from new localities from both the

*Corresponding author. Email: claudio.dicelma@unicam.it

Chilcatay and Pisco formations were collected and studied in detail (e.g. Bianucci, Lambert, & Post, 2010; Bianucci, Urbina, & Lambert, 2014; Ehret et al., 2012; Lambert, Bianucci, & de Muizon, 2008; Lambert, Bianucci, & Post, 2009, 2010; Lambert, Bianucci, Post, de Muizon, et al., 2010; Lambert, Bianucci, & Urbina, 2014; Lambert, de Muizon, & Bianucci, 2014, 2015). In the Ica desert, the Pisco Formation crops out as a series of small (up to ~200 m high), rounded hills called 'Cerros', most of which represent major fossil-bearing localities. At these sites, due to the arid climate and young uplift and exhumation, the stratigraphic section can be traced for several kilometres laterally, providing a unique opportunity to study how faunal assemblages changed through time, whether these changes coincided with palaeoenvironmental shifts, and what their nature might be. This type of study, however, requires strong spatial and temporal control over the stratigraphic succession, which can only be provided by the integration of refined stratigraphic data from section measuring, detailed geologic and structural field mapping, geochronological dating, and biostratigraphy. Unfortunately, despite the exceptional nature of the exposures and the limited structural deformation, stratigraphy and sedimentology of the important fossil-bearing localities of the Pisco Formation have only received cursory study, and just a few of them have been the subject of a more accurate stratigraphic investigation in recent years (Brand, Urbina, Chadwick, DeVries, & Esperante, 2011).

The large-scale (1:10,000) geological map and the associated stratigraphic section presented in this paper encompass the entire sedimentary succession of the Pisco Formation as exposed at Cerro Colorado. This study was carried out as part of a larger, ongoing project with a fivefold aim: (i) to provide strong stratigraphic control to some of the major fossiliferous localities of the Pisco Formation through the construction of detailed geological maps and the compilation of high-resolution stratigraphic sections; (ii) to establish the time interval represented by these deposits; (iii) to establish the depositional settings; (iv) to determine the faunal composition of major fossil localities; and (v) to confer accurate stratigraphic and time constraints to each fossil specimen through their correlation to the stratigraphic section and the absolute ages of the underlying and overlying ash layers. Essentially, this paper covers the first of the above-mentioned objectives for the Cerro Colorado fossil-bearing locality and represents the basis for future studies of the biological diversity of the Miocene vertebrate faunas. In a companion work to this study, Bianucci et al. (in press) establish the lateral and vertical distribution of fossil specimens within the same study area and provide some preliminary insights into the faunal changes that have occurred.

2. Geological setting

The Meso-Cenozoic tectonics of Peru were controlled by the convergence of the continental South American Plate and the oceanic Nazca/Farallon Plate. This tectonic collision developed a composite transform-convergent margin characterized by normal to strike slip faults that formed elongated extensional/pull apart basins along the Peruvian forearc (Dunbar, Marty, & Baker, 1990; Kulm, Resig, Thornburg, & Schrader, 1982; León, Aleman, Torres, Rosell, & De La Cruz, 2008; Zúñiga-Rivero, Klein, Hay-Roe, & Álvarez-Calderon, 2010) (Figure 1). The exposed portion of the Pisco basin extends along the narrow coastal plain of southern Peru from Pisco to Nazca towns and is located just landward of where the Nazca Ridge impinges on the Peru–Chile trench. The basement rocks are composed mostly of Precambrian gneiss and Lower Paleozoic granite covered by Upper Jurassic to Lower Cretaceous volcanics and sediments that, during Late Cretaceous–Early Tertiary time, formed a long and narrow structural high on the outer shelf of the Peru margin (Kulm et al., 1982; Thornburg & Kulm, 1981). To the east, the basin is bounded by the Coastal Batholith, a complex of igneous rocks mostly emplaced during the Late Cretaceous–early Eocene when arc magmatic activity was close to the location of the present coastline (Cobbing, 1999; Mukasa, 1986; Romero, Valencia, Alarcón, Peña, &

Figure 1. Map of the major structural trends and basins of coastal Peru, redrawn and modified from Travis, Gonzales, and Pardo (1976) and Thornburg and Kulm (1981).

Ramos, 2013 and references therein). As such, during deposition, the Pisco basin was a shallow-water, semi-enclosed embayment protected to the west by a chain of igneous islands of the emerging Outer-shelf Structural High (Marocco & Muizon, 1988; de Muizon & DeVries, 1985). Its clastic infill is about 2 km thick and has been subdivided into four main units that are, from the oldest to youngest, the Paracas Group, the Otuma Formation, the Chilcatay Formation, and the Pisco Formation (DeVries, 1998). Because these four units are bounded by three major breaks of the basin sedimentary record (DeVries, 1998) they can be defined as alloformations (North American Commission on Stratigraphic Nomenclature [NACSN], 2005). The basin fill succession shows extensive normal and transtensional faulting, which is the result of the strong coupling and prominent oblique convergence between the subducting oceanic slab and the overriding plate (León et al., 2008 and references therein). Rapid uplift and inversion of the basin started during late Pliocene time and record subduction of the aseismic Nazca Ridge (Hampel, 2002; Hsu, 1992; Macharé & Ortlieb, 1992; Pilger, 1981).

3. Study area and methods

The study area is located some 35 km southwest of the Ica town and covers an area of approximately 30 km^2 at Cerro Colorado, where an accurate field survey allowed the production of the attached 1:10,000-scale geological map (Main Map). The area was mapped during May and September 2014 as part of a multiyear mapping programme directed at producing complete geologic map coverage for some of the fossiliferous localities of the Pisco Formation. Three detailed sedimentary logs (Figure 2), here presented as a single composite stratigraphic column (see

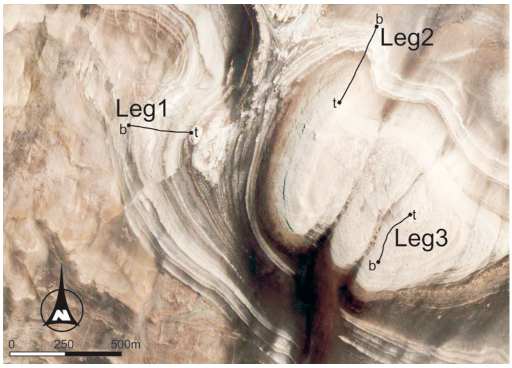

Figure 2. Google Earth image showing the locations of the three logged sections at Cerro Colorado. Log 1 is from the basal unconformity to the Quechua marker bed; Log 2 is from Quechua marker bed to the Ica-Chincha marker bed and ; Log 3 is from the Ica-Chincha marker bed to the top of the Cerro Colorado hill.

attached geological map), were measured at the decimetre scale through the exposed succession by using a Jacob's staff and taking into account the bedding attitude in terms of strike and dip.

The sediments transected by logs were described and sampled. For every single bed, lithology, colour, composition, texture, sedimentary structures, amount and type of bioturbation, palaeocurrent directions, and macrofossil content have been described. The stratigraphic analysis has been mainly carried out through the recognition and description of discontinuity surfaces. Both abrupt facies shifts and lithological contacts, in addition to the geometric relationships among the major geological bodies, have been used to recognize the discontinuities. The stratigraphic subdivision of the units confined by such discontinuities has been based on the criteria of the *allostratigraphic units* (NACSN, 2005). Due to their basinal spreading, the rank of alloformation boundary has been assigned to the interformational unconformities, whereas a rank of allomember boundary has been assigned to the intraformational unconformities. In order to further subdivide the unconformity-bounded stratigraphic units of the Pisco Formation into thinner sediment bodies, to successfully correlate them across the highly faulted study area, and to ensure a precise correlation and overlap of measured sections, eight local marker beds of different types and scattered throughout the exposed 200 m-thick succession have been identified, informally named, and physically tracked and mapped over distances of kilometres in the field.

Even though the stratigraphy of the Pisco Formation at Cerro Colorado is relatively simple, the presence of a complex fault network complicates attempts to compare laterally separated faunas through precise along-strike correlations. As a consequence, the study area required detailed geologic and structural mapping to identify its highly complex dispersed elements. Field mapping of these faults has been integrated with analysis of their geometry, kinematics, dimensional characteristics and quantification of fault displacements wherever possible in the field, and detailed interpretation of high-resolution Google Earth imagery.

Finally, in order to determine the relative ages of these strata, a number of bulk samples for biostratigraphic analysis purposes were collected at about 5 metre intervals.

4. Stratigraphic succession

The stratigraphic record exposed in the study area is divided into two distinct (allo)formations (Chilcatay Formation and Pisco Formation), in which the younger unit is structurally less deformed (Figure 2). Since this study was focused on specific aspects of the Pisco Formation, the underlying Chilcatay Formation was examined only in reconnaissance fashion during our field surveys and not mapped in the same detail as the Pisco Formation. As a consequence, it is not treated in detail here.

4.1. *The Chilcatay Formation*

The name Chilcatay Formation was assigned to late Oligocene to middle Miocene strata near Pampa Chilcatay, by Dunbar et al. (1990). The Chilcatay Formation consists of basal sandstones associated with a transgression at approximately 25 Ma (DeVries, 2001), tuffaceous and diatomaceous siltstone indicative of shelf depths and a coastal-upwelling regime (Dunbar et al., 1990), and intercalated coarse-grained sandstones that may represent short-lived early Miocene eustatic sea-level events (DeVries, 1998). Macharé and Fourtanier (1987) estimated the stratigraphic thickness of the Chilcatay Formation at approximately 250 m. In the study area a NW-striking, NE-facing monocline deforms the intensely faulted strata of the Chilcatay Formation, producing stratal dips of up to 15°.

4.2. *The Chilcatay–Pisco interformational unconformity*

The Chilcatay Formation is separated from the overlying Pisco Formation by a through-going, major angular unconformity recording rapid marine incursion (DeVries, 1998). In the study area, this surface is exposed between the northwestern and the southeastern corners of the map. Overall, contact relationships are difficult to observe due to a laterally extensive talus cover (Figure 3(a)). In the southern portion of the study area this unconformity is poorly exposed and consists of a cobble- to boulder-strewn surface. Elsewhere, such as in the northern portion of the study area, the boulder-rich interval is thin to absent and the contact appears as a sharp surface demarcated by a *Glossifungites* ichnofacies dominated by small, sharp-walled, and unlined *Thalassinoides* burrows. They penetrate at least 0.5 m into the underlying Chilcatay beds and are passively filled with coarse sands and granules infiltrated from the overlying transgressive lag (Figure 3(b)). Laterally, the firmground *Glossifungites* ichnofacies may grade into a *Trypanites* ichnofacies, demonstrating that the substrate was locally lithified.

This interformational unconformity is interpreted as a surface of subaerial exposure formed due to lowstand erosion and modified by a wave ravinement surface produced in the foreshore and upper shoreface during subsequent shoreline transgression and erosional shoreface retreat (e.g. Abbott, 1998; Cantalamessa, Di Celma, & Ragaini, 2006; Carnevale, Landini, Ragaini, Di Celma, & Cantalamessa, 2011; Di Celma & Cantalamessa, 2007; Nummedal & Swift, 1987; Zecchin & Catuneanu, 2013).

4.3. *The Pisco Formation*

Sediments of the Pisco Formation cover much of the map area and at Cerro Colorado make up a remarkably thick section spanning about 200 m of its basal portion. This stratigraphic section can be subdivided into two packages (allomembers) separated by an intraformational angular unconformity (Figure 4).

4.3.1. *Cerro Colorado lower allomember*

The lower allomember is estimated to be 75 m thick based on detailed geologic mapping and measured sections. Vertical progression of facies includes nearshore conglomerates and fine-grained sandstones grading upwards into offshore, thoroughly bioturbated sandy siltstones and

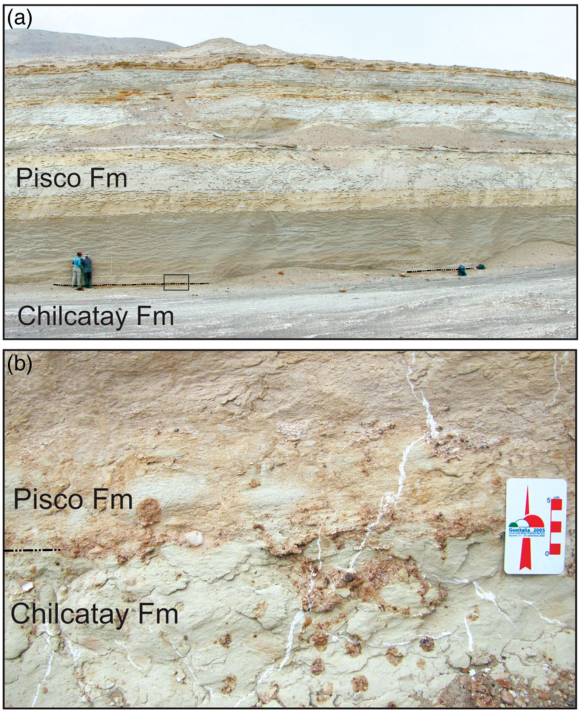

Figure 3. (a) Panoramic view of the unconformable contact (dash-double-dotted line) between the Chilcatay Formation and the overlying Pisco Formation (14°20′51.3″S-75°54′24.1″W). Geologists for scale and (b) closer view of the boxed area shown in (a) illustrating a detail of the contact. It is demarcated by a *Glossifungites* ichnofacies dominated by small *Thalassinoide*s descending at least 30 cm into the underlying beds and passively filled with coarse sands and granules infiltrated from the overlying transgressive lag.

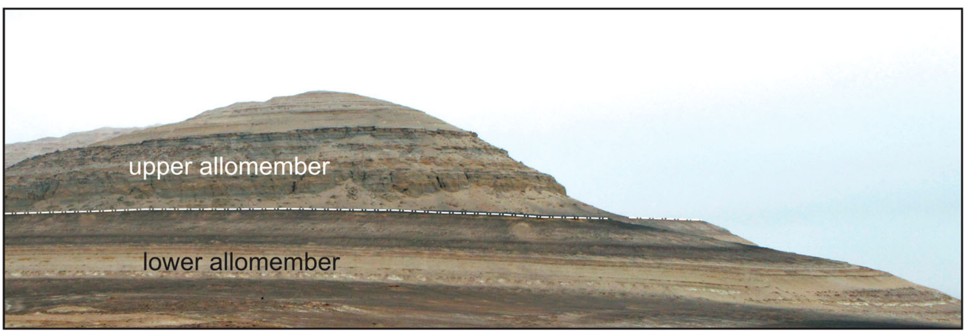

Figure 4. Panoramic field photo looking approximately northwest at the Pisco Formation. As viewed from a distance, rocks of the Cerro Colorado lower allomember are seen to dip approximately 10–12° to the NE, about 2–3° steeper than the gently dipping rocks of the upper allomember. This indicates the presence of a low-angle angular unconformity (white dot-dashed line) that formed by tilting and erosion of the lower allomember rocks, prior to deposition of upper allomember strata.

mudstones, and capped by biogenic deposits, including diatomites, diatomaceous mudstones and minor additions of sandstones, dolomitic horizons, and ash layers. Six volcanic ash layers have been identified in the lower allomember, with thickness ranging between 10 and 20 cm. These layers consist of coarse to fine ash. Some of them are white in colour and consist of volcanic glass shards only, in other cases they are creamy white to grey and contain a variable amount of juvenile biotite, feldspar, and quartz. The crystal fraction may be abundant, suggesting segregation during transport and settling. Lithic crystals and rock fragments, extraneous to the juvenile assemblage, are always present in variable amounts. Preliminary microanalytical data on glass shards of two ash layers indicate a rhyolitic composition of the volcanic glass and a high-K calcalkaline affinity.

The Cerro Colorado lower allomember is rich in vertebrate fossils and hosts almost all the vertebrate specimens identified to date (Bianucci et al., in press). Overall the structure of this unit is that of a moderately steep, faulted, NE-dipping monocline, with the exception of the south-eastern portion of the study area, where the immediate hanging wall of a NE-striking, SE-dipping strike fault with minor normal component is deformed into a fault-parallel, northeast plunging reverse drag fold. The anticline is intensely dissected and offset by high-angle, small-displacement, oblique normal faults and towards the northeast both the strike-slip fault and the associated anticline are draped by undeformed strata of the immediately overlying upper allomember.

Five major stratigraphic marker beds, representing a formidable tool to correlate isolated outcrops within the stratigraphic context of the Pisco Formation, have been defined throughout the Cerro Colorado study area. In ascending order they are the Nazca, Tiwanacu, Quechua, Wari, and Paracas marker beds. A brief description of each marker bed, including information on lithology and fossil content, is provided below.

Nazca marker bed. It is a 0.4 m-thick, tan to orange, fine-grained sandstone bed very well cemented by dolomite (Figure 5(a)). It tends to be emphasized in outcrop by differential erosion of resistant sandstone compared to the overlying erosionally recessive white diatomite.

Tiwanaku marker bed. It is composed of two nodular, 0.2 m-thick dolomite-cemented diatomite beds separated by a 10 cm-thick white diatomite bed. These beds are more resistant to erosion than the surrounding diatomites, producing ribs that weather in relief on the outcrop surfaces.

Quechua marker bed. This 1 m-thick, tan to orange sandstone bed is distinctive in outcrop because it is lithified and tends to stand out from the more easily eroded deposits around it, giving rise to prominent, laterally persistent ribs throughout the study area (Figure 5(b)).

Wari marker bed. A 0.8 m-thick, gray, massive, medium- to fine-grained sandstone bed (Figure 5(c). The upper portion of this bed is characterized by grit-filled spiral burrows of the ichnogenus *Gyrolithes vidali* (Muñiz, Esperante, & Poma, 2011) that penetrate to depths of as much as 0.4 m (Figure 5(d)).

Paracas marker bed. It is a lithologically distinctive package of beds as much as 1.4 m thick that weathers to form a laterally persistent low cliff (Figure 5(e)). Near the base it consists of an interval of thinly bedded, tan to orange streaked diatomaceous siltstones with a 5 cm-thick laterally persistent purple bed. This lower portion passes upward into a 0.5 m-thick interval characterized by small-scale, diatomite-filled scours up to 0.4 m high and up to 1 m wide that, in turn, is capped by a 0.25 m-thick, grey, fine-grained sandstone bed overlain by a tan to orange, well-indurated siltstone bed 0.2–0.25 m thick (Figure 5(f)). In panoramic views this marker bed is conspicuous by its colour, generally slightly darker than the surrounding sediments.

4.3.2. *The Pisco Formation intraformational unconformity*

An angular unconformity within the Pisco Formation strata separates the lower allomember from the overlying upper allomember. This surface, forming one of the most prominent benches in the study area, can be followed all around the Cerro Colorado hill and along the northern and eastern sides of the study area. The erosional episode represented by this unconformity has removed variable amounts of underlying sediments. At the outcrop scale, it is a knife-sharp and irregular

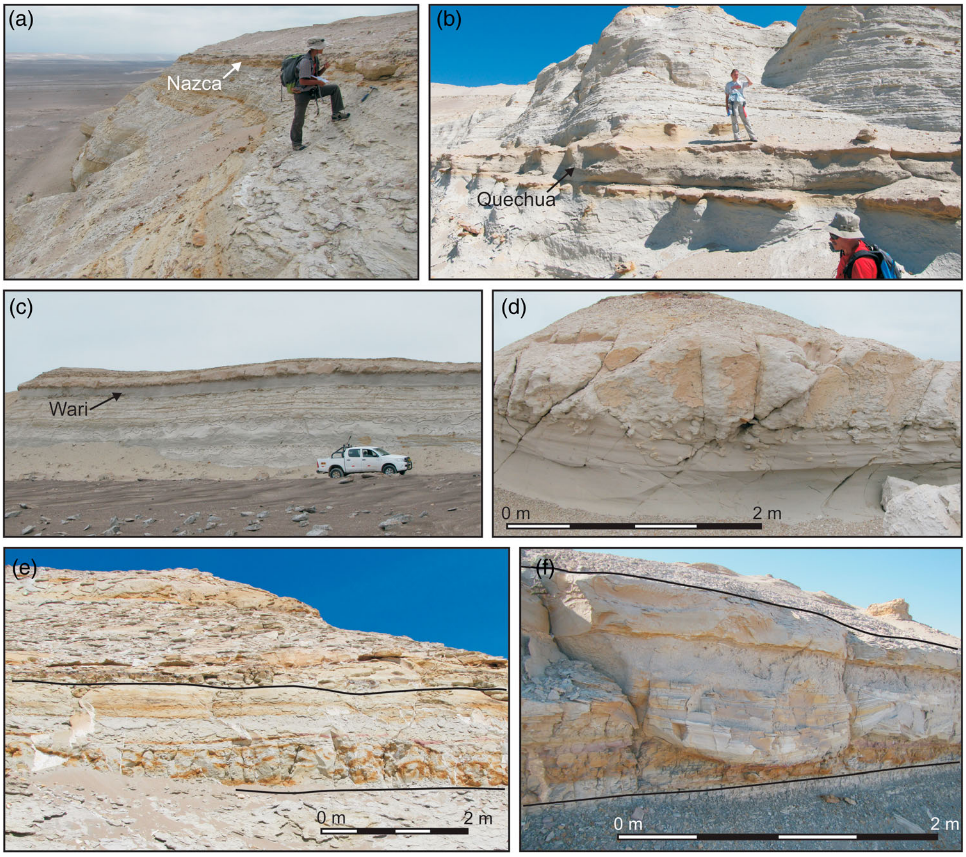

Figure 5. Outcrop photographs of the marker beds in the lower allomember. (a) Detail of the Nazca sandstone marker bed at 14°20′51.3″S-75°54′24.1″W; (b) close-up of the Quechua sandstone marker bed at 14°20′32.7″S-75°54′06.0″W; (c) panoramic view and (d) detail of the Wari marker bed at14°22′10″S-75°52′40.57″W; (e) panoramic view of the Paracas marker bed at 14°20′40.4″S-75°53′46.3″W; and (f) detail of the Paracas marker bed showing multiple infill of a small, shallow cut-and-fill structure that is typically filled by thinly bedded diatomite layers characterized by rapid lateral thinning and then pinching out.

surface-forming undulations that never exceed 0.5 m of relief and typically defined by a 0.3 m-thick, shell-rich gravel facies sharply overlying truncated beds of the lower allomember (Figure 6(a)). Clasts range from well-rounded small pebbles to small boulders and consist of igneous rocks and dolomitized siltstone penetrated by rock-boring pholad bivalves (Figure 6(b)). These molluscs are locally abundant, and often preserved *in situ,* with valves adjoined. The evidence summarized above is consistent with an unconformity representing a co-planar surface formed due to amalgamation of erosion during both a relative sea-level lowstand and the subsequent landward passage of the shoreface of a transgressing sea (e.g. Abbott, 1998; Cantalamessa et al., 2006; Carnevale et al., 2011; Di Celma & Cantalamessa, 2007; Nummedal & Swift, 1987; Zecchin & Catuneanu, 2013).

4.3.3. *Cerro Colorado upper allomember*

This stratigraphic unit is as much as 125 m thick and its strata are exposed in the upper half of the Cerro Colorado hill and along the northern and eastern portions of the study area. Overall its

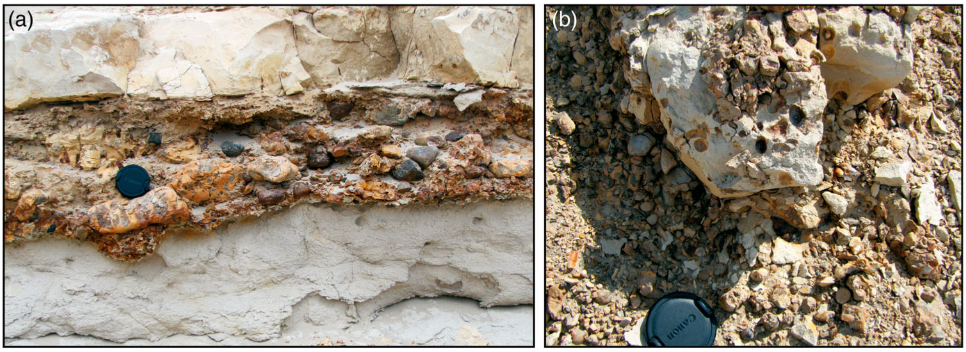

Figure 6. Details of the intraformational unconformity. A lens cap (6.5 cm in diameter) is used for scale. (a) The unconformity consists of an irregular erosional surface covered by a 0.3 m-thick transgressive lag produced by ravinement and consisting of clasts of both igneous and sedimentary rocks and moulds of molluscs and (b) most of the sedimentary clasts from the conglomerate contain abundant, clavate-shaped, dwelling borings produced by pholad bivalves.

structure is that of a very gentle (4–6°), NNE-dipping homocline. Fossil vertebrates are relatively less frequent with respect to the lower allomember, and mainly consists of remains of large baleen whales and pinnipeds (Bianucci et al., in press). The Cerro Colorado upper allomember can be subdivided into two main lithological packages separated by the Inca marker bed. The lower package, up to 50 m thick, consists of grey and orange, very fine- to medium-grained sandstones displaying abundant evidence of current and wave reworking, including large and fine-scale cross-bedding and swaley cross-stratification (Leckie & Walker, 1982). Palaeocurrent measurements reveal significant scatter, with overall transport to the northeast. The upper package, as much as 75 m thick, is mostly composed of finely laminated grey–white diatomite with minor additions of sandstones, dolomitic horizons, ash layers, and slump deposits, suggesting that a major change in sedimentary facies takes place across the Inca marker bed, from shallow marine tractionites below to deeper marine, suspension-emplaced biogenic mudstone above.

The 17 volcanic ash layers identified in this unit show highly variable thickness, ranging from 5 to 200 cm, and composition. They are mainly unconsolidated, but some are cemented by minerals of diagenetic or supergenic origin. Several contain a high fraction of non-juvenile clasts, such as rounded reddish quartz crystals, altered volcanic clasts and crystals, diatoms. Some layers, instead, can be considered representative of a distal water-settled fallout, since they are almost entirely composed of glass shards with scarce biotite and feldspar crystals and minor non-juvenile material. The uppermost ash layer can be subdivided into a lower, biotite-bearing interval, and an upper biotite-free interval. Despite the volcanic origin of most components, it has heterogeneous crystal assemblage (quartz, feldspars, biotite, pyroxene, olivine, Fe-oxides) suggesting processes of reworking of volcanogenic material of marine or/and continental deposition. Preliminary microanalytical data on the glass shards of two layers indicate a high-silica rhyolitic composition and a high-K calcalkaline affinity.

Three major marker beds that are readily traceable throughout the map area have been distinguished in the Cerro Colorado upper allomember. They are, from youngest to oldest, the Inca, the Ica-Chincha, and the T17 marker beds (Figure 7(a)).

Inca. It is the highest of a set of brown to tan, fine-grained sandstone beds strongly cemented with dolomite. It is 0.5 m thick and forms prominent ledges or benches around the Cerro Colorado hill (Figure 7(b)). In cross-sectional view it displays a rather dense network of *Thalassinoides* burrows (Figure 7(c)), whereas its upper surface contains large numbers of moulds of articulated *Dosinia* bivalves.

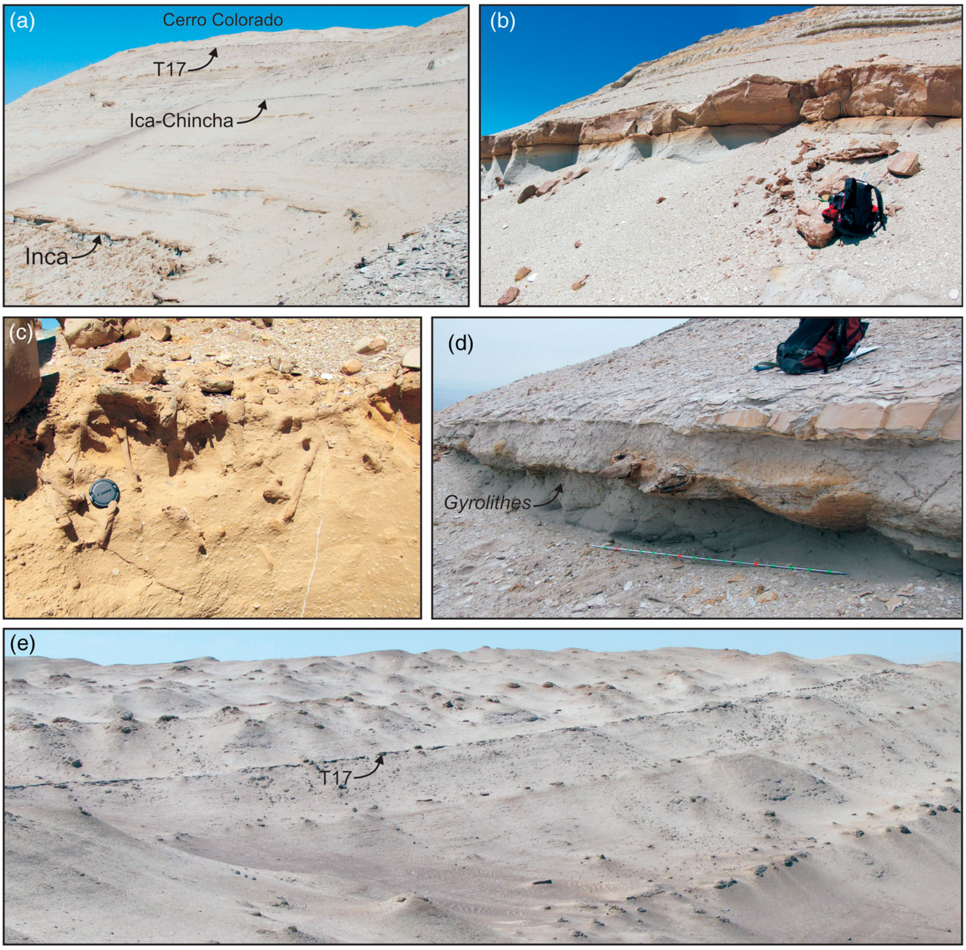

Figure 7. (a) Panoramic view of the northeastern side of Cerro Colorado showing the three marker beds in the upper allomember; (b) detail of the more resistant Inca marker bed standing out of the weathered surface and (c) frequently bioturbated by *Thalassinoides* burrows; (d) close-up view of the Ica-Chincha sandstone marker beds showing silicified wood logs and *Gyrolithes* burrows; and (e) panoramic view of the T17 marker bed.

Ica-Chincha. A grey, massive, medium-grained sandstone bed with spiral burrows perpendicular to the bedding plane that may be referred to the ichnogenus *G. vidali* (Muñiz et al., 2011). Its thickness is not constant throughout the study area and ranges between 0.8 and 1.4 m (Figure 7(d)).

T17. It is a 0.3 m-thick grey ash layer overlain by a 0.2 m-thick dolomitized siltstone bed forming a fairly continuous and prominent bench along the southwestern side of the Cerro Colorado hill (Figure 7(e)).

5. Biostratigraphic framework

Although the Pisco Formation has mostly been deposited under upwelling conditions (Suess & von Huene, 1988), microfloristic assemblages at Cerro Colorado are typical of neritic environments. Coastal, epiphytic, and psammophil diatom genera, such as *Delphineis*, *Odontella*, *Rhaphoneis*, and *Diplomenora*, are common in both the lower and upper allomembers, whereas outer shelf and open-ocean stratigraphic-meaningful diatom species are less common. Nevertheless, a few samples containing widely distributed diatom taxa allow a preliminary biostratigraphic constraint. The lower allomember is assigned to subzone D of the *Denticulopsis hustedtii*– *Denticulopsis lauta* zone (middle- to high-latitude zonation of Barron, 1985), based on the co-occurrence of *D. hustedtii* and *Lithodesmium reynholdsii* within samples from about 1 and 3 m above the Nazca and Wari marker beds, respectively, indicating a late Miocene age. The top of the upper allomember is not older than Subzone B of the *D. hustedtii* zone of Barron (1985), based on the occurrence of *Thalassiosira antiqua* in a sample at the top of the Cerro Colorado Section. In fact, *T. antiqua* appears within this zone, but its record extends up to late Pliocene: therefore the top of the upper allomember is at least late Miocene in age but could be younger. Based on these data, more detailed biostratigraphic studies are needed to better constrain the age of the upper allomember and the time gap corresponding to the intraformational unconformity.

6. Structural analysis

The sedimentary succession exposed in the Cerro Colorado area is dissected by faults varying in kinematics from extensional to strike-slip and affecting both the Chilcatay and Pisco Formations. The large majority of the identified faults are quite small normal faults that have a few metres of stratigraphic throw, as determined from the vertical offset of the marker beds (Figure 8). However, some of these faults have normal displacement up to 10–15 m. Normal faults display two main ranges of orientations, with the majority of faults N160°–10°E striking and the remainder generally N70°–100°E striking. Dip angles of the faults are mostly comprised between 65 and 75°. Striations indicate that all of the faults are either pure normal faults or have a minor strike-slip

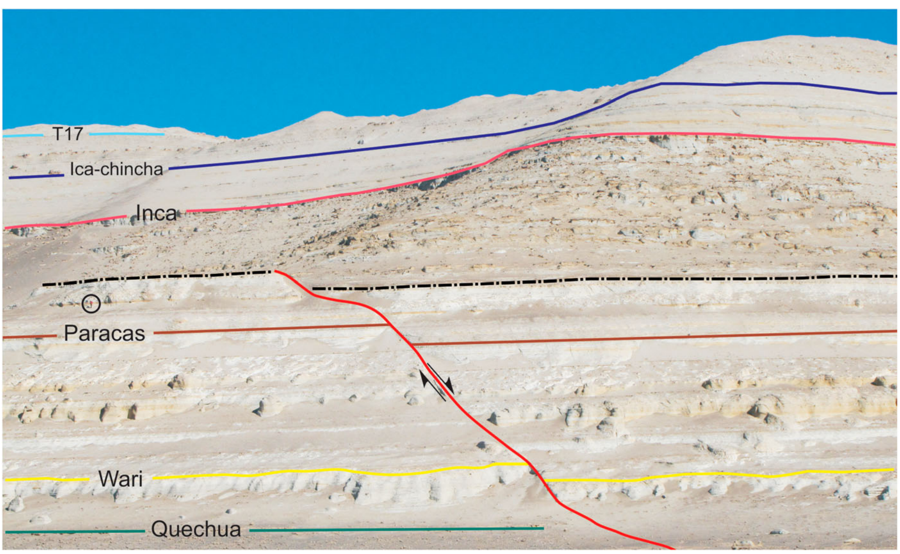

Figure 8. Panoramic view of the eastern side of Cerro Colorado (14°20′38″S-75°53′50″W) showing one of the small-displacement normal faults in the area offsetting some of the main marker beds (coloured lines), and the intraformational unconformity (black dot-dashed line). View is to the southwest. Circled person for scale.

component of motion, which is left-lateral for the N160°–10°E striking faults and right-lateral for those striking N70°–100°E. Mutual abutting and cross-cutting relationships between normal faults significantly varying in strike, up to mutually orthogonal, suggest the penecontemporaneous activity of all the normal faults.

A few strike-slip faults are clustered as a major fault zone at the southeastern corner of the map, where they form an array of aligned and linked faults with associated folding. Faults strike generally N35°–55°E and dip 70–85° mainly to the southeast. Overall, the fault zone is at least 3 km long and cuts the Chilcatay Formation and the lower allomember of the Pisco Formation, but is sealed by overlying strata of the upper allomember. The fault zone displays approximately 500 m of right separation based on horizontally offset marker beds, as well as a secondary and minor southeast-down normal displacement estimated in 45 m from the geological cross-section. Weak fault zone reactivation with a left-lateral component of motion is suggested by both field kinematic indicators and by a less than 10 m horizontally displaced normal fault. Since normal faults were not involved in folding associated with activity of the strike-slip faults, the latter are older than the former. Only the probable reactivation of the strike-slip faults with a left-lateral sense of motion could be compatible with a penecontemporaneous activity of the normal faults.

7. Conclusions

The 200 m-thick section of the Pisco Formation exposed at Cerro Colorado has been investigated for detailed lithology, correlation, and structural features. The geological mapping revealed two important angular unconformities. The first one is the interformational basal unconformity between the Chilcatay Formation and the overlying Pisco Formation. The second one is a low-angle intraformational discontinuity that allowed the subdivision of the Pisco stratigraphy into two informal allomembers. Dating of the exposed succession by diatom biostratigraphy suggests that the age of the lower allomember is late Miocene, whereas the upper allomember is late Miocene or younger.

To tightly constrain the Pisco stratigraphy and geological structure and to facilitate correlations, eight marker beds have been defined, which can be easily traced laterally throughout the outcrop belt and provide a detailed understanding of the local geology. The investigated portion of the Pisco Formation is a gently dipping, northeast-facing monocline. Accurate mapping of the fault network, both in the field and from aerial photography, provided insight into its organization and shows three dominant sets of high-angle normal to strike-slip faults of relatively small displacement.

Acknowledgements

Journal reviewers Massimo Zecchin, Leonard Brand, Gelson Luís Fambrini, John Abraham and Associate Editor Claudio Riccomini are gratefully acknowledged for their thoughtful contribution and helpful criticism that sharpened the focus of this study. Last, but not least, C.D.C. would like to thank his wife Desy and his two lovely children Marco and Sveva for their endless patience during the long periods he spent in the field. The logistics of fieldwork were greatly assisted by Mario Urbina (Museo de Historia Natural, Universidad Nacional Mayor de San Marcos, Lima).

Disclosure statement

No potential conflict of interest was reported by the author(s).

Funding

This study was supported by grants from the Italian Ministry of University and Research to Bianucci (PRIN Project, 2012YJSBMK EAR-9317031), Malinverno (PRIN Project, 2012YJSBMK_002), Di Celma (PRIN Project, 2012YJSBMK_003), and National Geographic Society Committee on Research Exploration to Bianucci (9410–13).

Software

The geological map and associated geological sections were compiled by scanning hand drafts as black and white TIF files, and then digitizing the linework using the Corel Draw X3 graphics package. By using the GIS Data processing application Global Mapper 12, contour lines for the 1:10,000 scale topographic base map were generated from digital elevation models (DEMs) based on the Shuttle Radar Topography Mission 26 (SRTM) as released by the United States Geological Survey (SRTM3 USGS version 2.1).

References

Abbott, S. T. (1998). Transgressive systems tract and onlap shellbeds from Mid Pleistocene sequences, Wanganui Basin, New Zealand. *Journal of Sedimentary Research*, *68*, 253–268.

Barron, J. A. (1985). Miocene to Holocene planktic diatoms. In H. M. Bolli, J. B. Saunders, & K. P. Perch-Nielsen (Eds.), *Plankton stratigraphy* (pp. 763–809). Cambridge: Cambridge Univ. Press.

Bianucci, C., Di Celma, C., Landini, W., Post, K., Tinelli, C., de Muizon, C., … Lambert, O. (in press). Distribution of fossil marine vertebrates in Cerro Colorado, the type locality of the giant raptorial sperm whale *Livyatan melvillei* (Miocene, Pisco Formation, Peru). *Journal of Maps*. Retrieved from http://dx.doi.org/10.1080/17445647.2015.1048315

Bianucci, G., Lambert, O., & Post, K. (2010). High concentration of long-snouted beaked whales (genus *Messapicetus*) from the Miocene of Peru. *Palaeontology*, *53*, 1077–1098.

Bianucci, G., Urbina, M., & Lambert, O. (2014). A new record of *Notocetus vanbenedeni* (Squalodelphinidae, Odontoceti, Cetacea) from the early Miocene of Peru. *Comptes Rendus Palevol.*, *14*, 5–13.

Brand, L., Urbina, M., Chadwick, A., DeVries, J. T., & Esperante, R. (2011). A high resolution stratigraphic framework for the remarkable fossil cetacean assemblage of the Miocene/Pliocene Pisco Formation, Peru. *Journal of South American Earth Sciences*, *31*, 414–425.

Cantalamessa, G., Di Celma, C., & Ragaini, L. (2006). Tectonic controls on sequence stacking pattern and along-strike architecture in the Pleistocene Mejillones Formation, northern Chile: Implications for sequence stratigraphic models. *Sedimentary Geology*, *183*, 125–144.

Carnevale, G., Landini, W., Ragaini, L., Di Celma, C., & Cantalamessa, G. (2011). Taphonomic and paleoecological analyses (mollusks and fishes) of the Sua Member condensed shellbed, Upper Onzole Formation (early Pliocene, Ecuador). *PALAIOS*, *26*, 160–172.

Cobbing, E. J. (1999). The Coastal Batholith and other aspects of Andean magmatism in Peru. In A. Castro, C. Fernandez, & J. L. Vigneresse, (Eds.), *Understanding granites: Integrating new and classical techniques* (pp. 111–122). London: Geological Society, Special Publications, 168.

DeVries, T. J. (1998). Oligocene deposition and Cenozoic sequence boundaries in the Pisco Basin (Peru). *Journal of South American Earth Sciences*, *11*, 217–231.

DeVries, T. J. (2001). Molluscan evidence for an Oligocene-Miocene age of 'Paracas' beds in southern Peru. *Boletin de la Sociedad Geológica del Perú*, *92*, 57–65.

Di Celma, C., & Cantalamessa, G. (2007). Sedimentology and high-frequency sequence stratigraphy of a forearc extensional basin: The Miocene Caleta Herradura Formation, Mejillones Peninsula, northern Chile. *Sedimentary Geology*, *198*, 29–52.

Dunbar, R. B., Marty, R. C., & Baker, P. A. (1990). Cenozoic marine sedimentation in the Sechura and Pisco basins, Peru. *Palaeogeography, Palaeoclimatology, Palaeoecology*, *77*, 235–261.

Ehret, D. J., Mac Fadden, B. J., Jones, D. S., DeVries, T. J., Foster, D. A., & Salas-Gismondi, R. (2012). Origin of the white shark Carcharodon (Lamniformes: Lamnidae) based on recalibration of the upper Neogene Pisco Formation of Peru. *Paleontology*, *55*, 1139–1153.

Hampel, A. (2002). The migration history of the Nazca Ridge along the Peruvian active margin: A re-evaluation and some geological implications. *Earth and Planetary Science Letters*, *203*, 665–679.

Hsu, J. T. (1992). Quaternary uplift of the Peruvian coast related to the subduction of the Nazca Ridge: 13.5 to 15.6 degrees south latitude. *Quaternary International*, *15/16*, 87–97.

Kulm, L. D., Resig, J. M., Thornburg, T. M., & Schrader, H. J. (1982). Cenozoic structure, stratigraphy and tectonics of the central Peru forearc. In J. K. Legget (Ed.), *Trench and forearc geology: Sedimentation and tectonics on modern and ancient plate margins* (pp. 151–169). London: Blackwells.

Lambert, O., Bianucci, G., & Beatty, B. L. (2014). Bony outgrowths on the jaws of an extinct sperm whale support macroraptorial feeding in several stem physeteroids. *Naturwissenschaften*, *101*, 517–521.

Lambert, O., Bianucci, G., & de Muizon, C. (2008). A new stem-sperm whale (Cetacea, Odontoceti, Physeteroidea) from the latest Miocene of Peru. *Comptes Rendus Palevol*, *7*, 361–369.

Lambert, O., Bianucci, G., & Post, K. (2009). A new beaked whale (Odontoceti, Ziphiidae) from the Middle Miocene of Peru. *Journal of Vertebrate Paleontology*, *29*, 910–922.

Lambert, O., Bianucci, G., & Post, K. (2010). Tusk-bearing beaked whales from the Miocene of Peru: Sexual dimorphism in fossil ziphiids? *Journal of Mammalogy*, *91*, 19–26.

Lambert, O., Bianucci, G., Post, K., de Muizon, C., Salas-Gismondi, R., Urbina, M., & Reumer, J. (2010). The giant bite of a new raptorial sperm whale from the Miocene epoch of Peru. *Nature*, *466*, 105–108.

Lambert, O., Bianucci, G., & Urbina, M. (2014). *Huaridelohis raimondii*, a new early Miocene Squalodelphinidae (Cetacea, odontoceti) from the Chilcatay Formation, Peru. *Journal of Vertebrate Paleontology*, *34*, 987–1004.

Lambert, O., de Muizon, C., & Bianucci, G. (2014). The most basal beaked whale *Ninoziphius platyrostris* Muizon, 1983: clues on the evolutionary history of the family Ziphiidae (Cetacea: Odontoceti). *Zoological Journal of the Linnean Society*, *167*, 569–598.

Lambert, O., de Muizon, C., & Bianucci, G. (2015). A new archaic homodont toothed whale (Mammalia, Cetacea, Odontoceti) from the early Miocene of Peru. *Geodiversitas*, *37*, 79–108.

Leckie, D. A., & Walker, R. G. (1982). Storm- and tidedominated shorelines in Cretaceous Moosebar–Lower Gates interval—outcrop equivalents of deep basin gas trap in Western Canada. *Bulletin of the American Association of Petroleum Geologists*, *66*, 138–157.

León, W., Aleman, A., Torres, V., Rosell, W., & De La Cruz, O. (2008). Estratigrafía, Sedimentología y evolución tectónica de la cuenca Pisco Oriental. *Boletín INGEMMET*, *27*(Serie D), pp. 144, Lima, Peru.

Macharé, J., & Fountanier, E. (1987). Datations des formations tertiaires du bassin de Pisco (Pérou) à partir d'associations de diatomées. *Comptes Rendus de l'Académie des Sciences Paris*, t. *305*(Série 2), 407–412.

Macharé, J., & Ortlieb, L. (1992). Plio-Quaternary vertical motions and the subduction of the Nazca Ridge, central coast of Peru. *Tectonophysics*, *205*, 97–108.

Marocco, R., & de Muizon, C. (1988). Le Bassin Pisco, bassin cénozoïque d'avant arc de la côte du Pérou central: analyse géodynamique de son remplissage. *Géodynamique*, *3*, 3–19.

de Muizon, C., & DeVries, T. J. (1985). Geology and paleontology of late Cenozoic marine deposits in the Sacaco area (Peru). *Geologische Rundschau*, *74*, 547–563.

Mukasa, S. B. (1986). Zircon U–Pb ages of super-units in the Coastal Batholith, Peru: Implications for magmatic and tectonic processes. *Geological Society of America Bulletin*, *97*, 241–254.

Muñiz, F., Esperante, R., & Poma, O. (2011). *La ichnospecie Gyrolithes vidali mayoral 1986 en al Mioceno superior de la Formacixn Pisco (Ica, Perù)*. Implicaciones paleoambientales. Abstract volume of the XXVII Jornadas de la Sociedad Española de Paleontología, Sabadell (Barcelona), Spain, 263–267.

North American Commission on Stratigraphic Nomenclature. (2005). North American stratigraphic code. *American Association of Petroleum Geologists Bulletin*, *89*, 1547–1591.

Nummedal, D., & Swift, D. J. P. (1987). Transgressive stratigraphy at sequence bounding unconformities: Some principles derived from Holocene and Cretaceous examples. In D. Nummedal, O. H. Pilkey, & J. D. Howard (Eds.), *Sea-level fluctuation and coastal evolution* (pp. 241–260). Tulsa: SEPM. Special Publication, 41.

Pilger, R. H. (1981). Plate reconstructions, aseismic ridges, and low-angle subduction beneath the Andes. *Geological Society of America Bulletin*, *92*, 448–456.

Romero, D., Valencia, K., Alarcón, P., Peña, D., & Ramos, V. A. (2013). The offshore basement of Perú: Evidence for different igneous and metamorphic domains in the forearc. *Journal of South American Earth Sciences*, *42*, 47–60.

Suess, E., & von Huene, R. (1988). Introduction, objectives, and principal results, Leg 112, Peru continental margin. *Proc. Ocean Drilling Program, Init. Rep.*, *112*, 5–44.

Thornburg, T. M., & Kulm, L. D. (1981). Sedimentary basins of the Peru continental margin: structure, stratigraphy, and Cenozoic tectonics from 6°S to 16°S latitude. In L. D. Kulm, J. Dymond, E. J. Dasch, & D. M. Hussong, (Eds.), *Nazca plate: crustal formation and Andean convergence* (pp. 393–422). Boulder, CO: *Geological Society of America*, Memoir *154*.

Travis, R. B., Gonzales, G., & Pardo, A. (1976). Hydrocarbon potential of coastal basins of Peru. In M. Halbouty, J. Maher, & H. M. Lian, (Eds.), *Circum-pacific energy and mineral resources* (Vol. 25, pp. 331–338). Tulsa: American Association of Petroleum Geologists Memoir.

Zecchin, M., & Catuneanu, O. (2013). High-resolution sequence stratigraphy of clastic shelves I: Units and bounding surfaces. *Marine and Petroleum Geology*, *39*, 1–25.

Zúñiga-Rivero, F. J., Klein, G. D., Hay-Roe, H., & Álvarez-Calderon, E. (2010). *The hydrocarbon potential of Peru*. Lima: BPZ Exploración & Producción S.R.L., 338 p.